Supplementary material for LHCb-PAPER-2019-024

A Comparison of the η_c mass measurements

A comparison of the current measurement of the J/ψ and η_c mass difference with previous measurements is shown in Fig. 1.

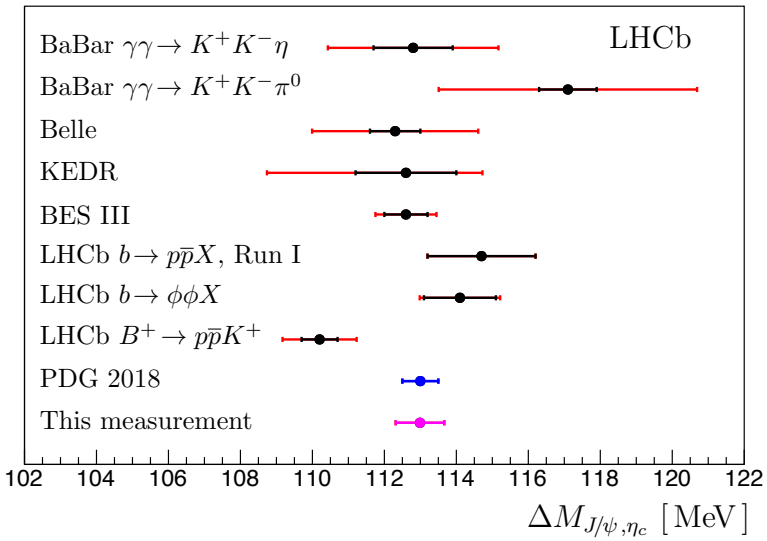

Figure 1: Measurement of mass difference $\Delta M_{J/\psi,\eta_c}$ compared to measurements from BaBar [1], Belle [2], KEDR [3], BES III [4] and LHCb [5–7]; black error bars represent statistical uncertainties, red error bars represent total uncertainties. The blue point with error bar shows the world average [8], the magenta point with error bars represents the current measurement.

B Comparison with theory prediction

The comparison of the measured η_c differential prompt production cross-section with the colour-singlet model prediction [9] is shown in Fig. 2. While the colour-singlet contribution provides in general a good description of the LHCb measurements, an indication of a different slope could point to a colour-octet contribution exhibiting at larger $p_{\rm T}$ values. Enlarging measured $p_{\rm T}$ range and improving theory uncertainties can be decisive to quantify this effect.

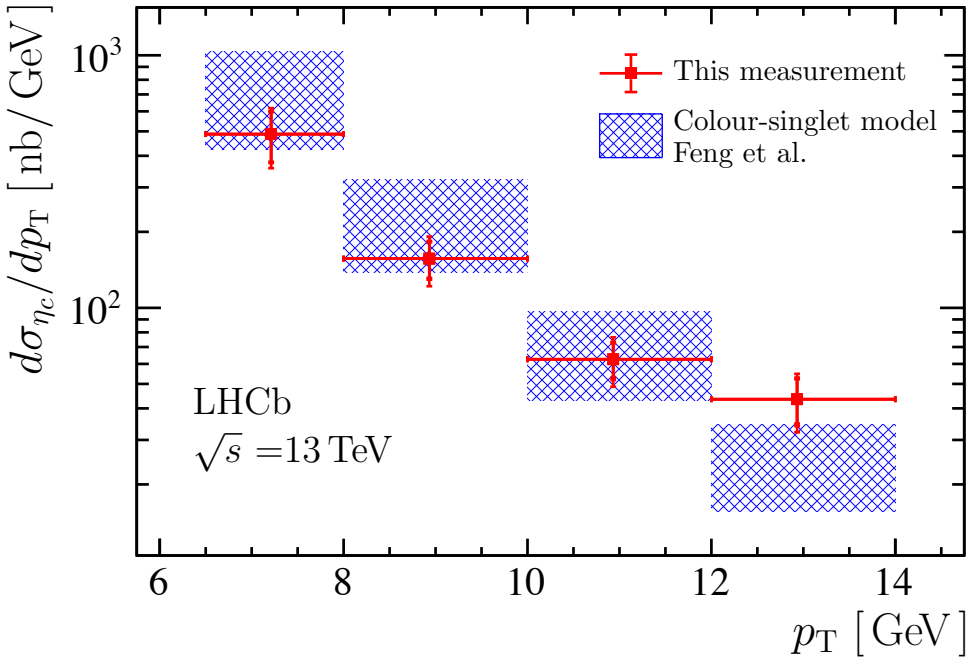

Figure 2: Measured (points) prompt production cross-section of the η_c meson compared to the prediction (boxes) of the colour-singlet model [9].

C Fit to the invariant mass in bins of p_{T}

Projections of simultaneous fits to prompt-enriched and b-hadron-enriched samples in p_{T} bins are shown in Figs. 3, 4, 5 and 6. The signal yields after background subtraction are displayed below the corresponding projections. In general, the fit gives a good description of all $M_{p\overline{p}}$ distributions.

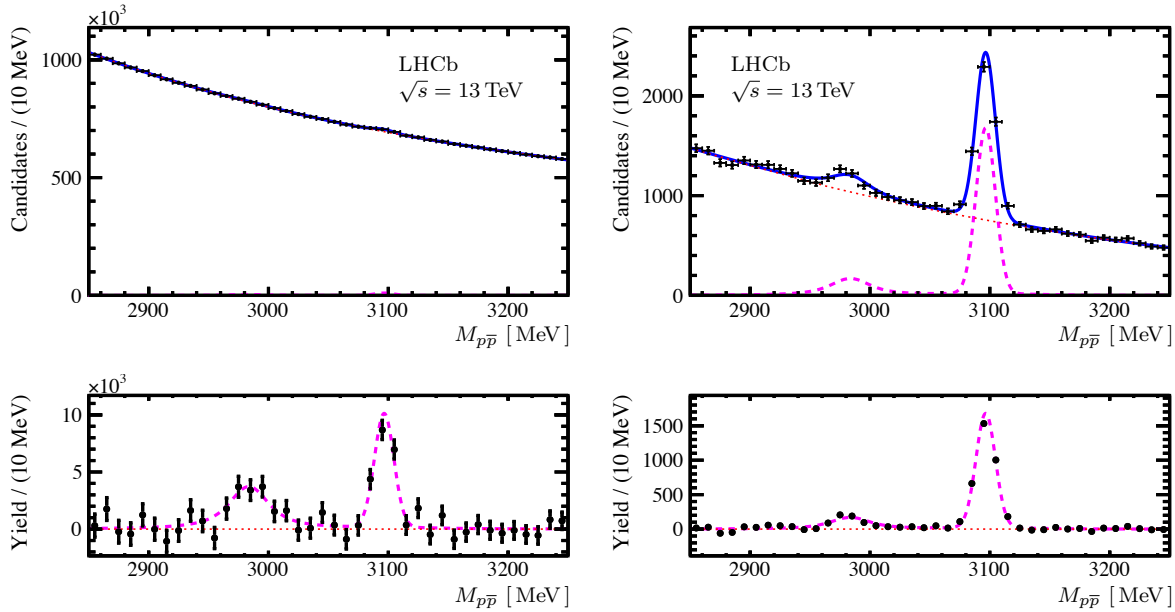

Figure 3: Invariant mass distribution of the $p\overline{p}$ candidates for (top left) prompt enriched and (top right) b-hadron enriched samples in the p_{T} range $6.5 < p_{\mathrm{T}} < 8.0\,\mathrm{GeV}$. The solid blue lines represent the total fit result. The dashed magenta and dotted red lines show the signal and background components, respectively. Signal distributions with subtracted background components from the fit are shown on the bottom plots for the two samples, respectively.

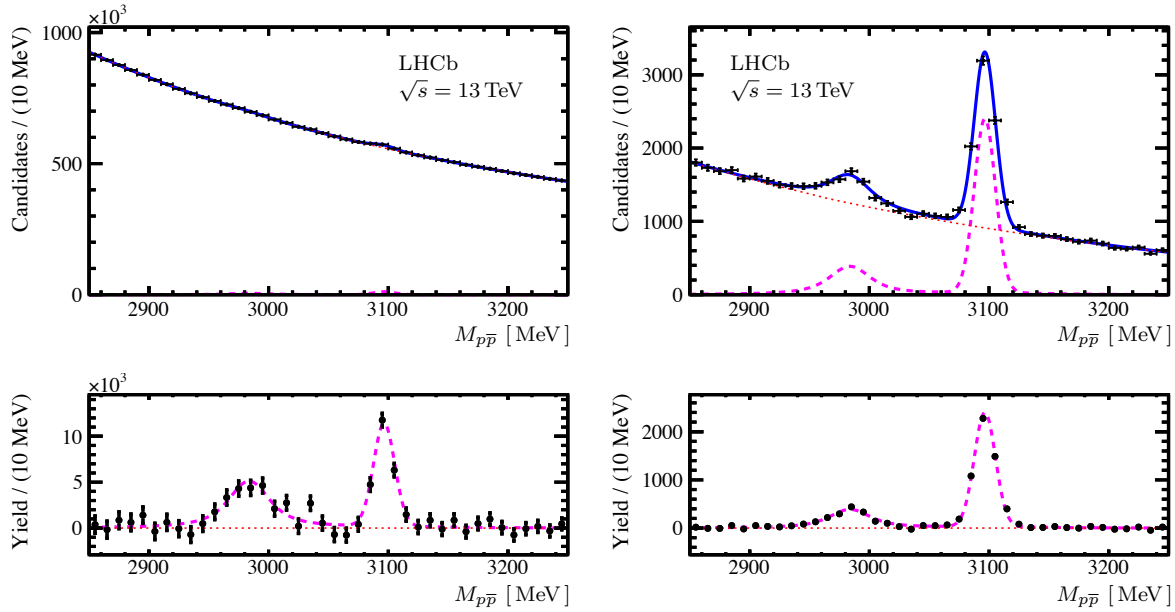

Figure 4: Invariant mass distribution of the $p\overline{p}$ candidates for (top left) prompt enriched and (top right) b-hadron enriched samples in the p_{T} range $8.0 < p_{\mathrm{T}} < 10.0\,\mathrm{GeV}$. The solid blue lines represent the total fit result. The dashed magenta and dotted red lines show the signal and background components, respectively. Signal distributions with subtracted background components from the fit are shown on the bottom plots for the two samples, respectively.

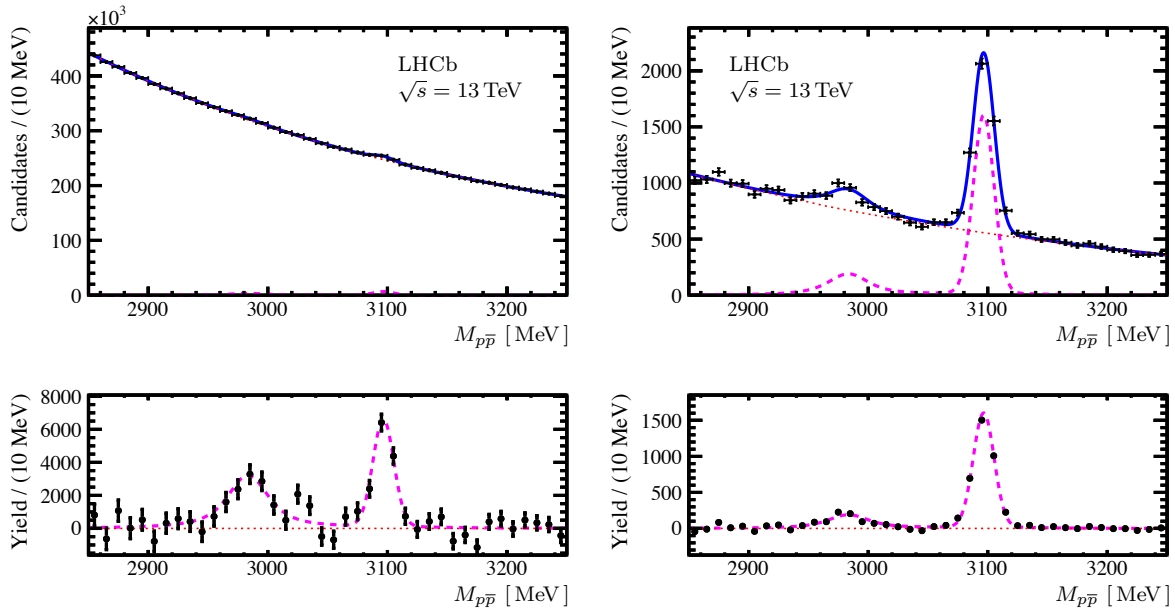

Figure 5: Invariant mass distribution of the $p\overline{p}$ candidates for (top left) prompt enriched and (top right) b-hadron enriched samples in the p_{T} range $10.0 < p_{\mathrm{T}} < 12.0\,\mathrm{GeV}$. The solid blue lines represent the total fit result. The dashed magenta and dotted red lines show the signal and background components, respectively. Signal distributions with subtracted background components from the fit are shown on the bottom plots for the two samples, respectively.

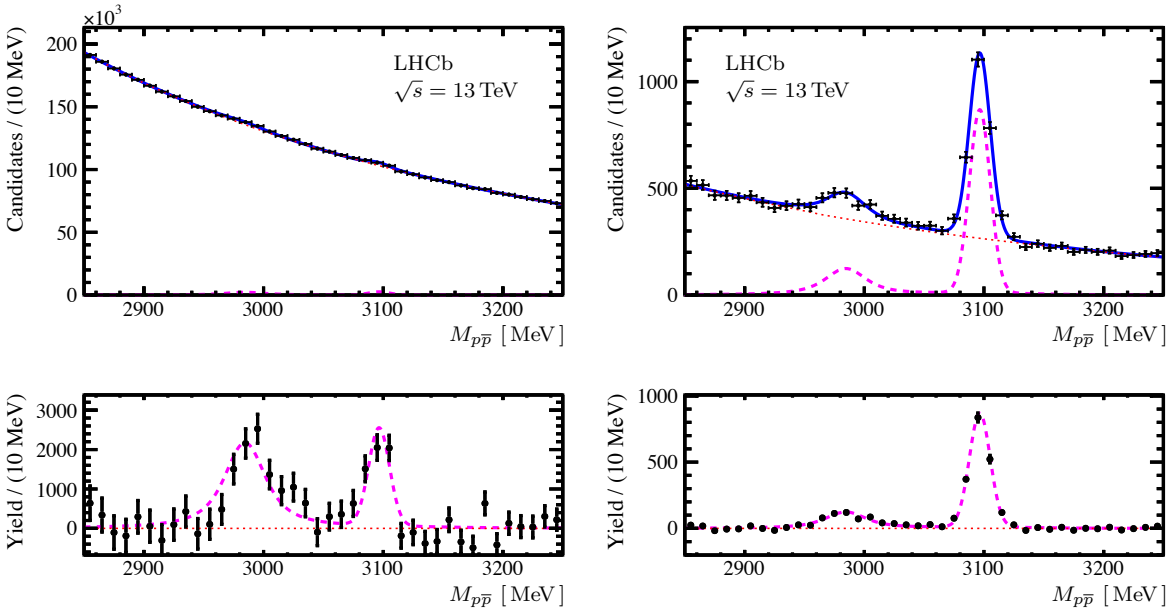

Figure 6: Invariant mass distribution of the $p\overline{p}$ candidates for (top left) prompt enriched and (top right) b-hadron enriched samples in the p_{T} range $12.0 < p_{\mathrm{T}} < 14.0\,\text{GeV}$. The solid blue lines represent the total fit result. The dashed magenta and dotted red lines show the signal and background components, respectively. Signal distributions with subtracted background components from the fit are shown on the bottom plots for the two samples, respectively.

References

[1] BaBar collaboration, J. P. Lees *et al.*, *Dalitz plot analysis of $\eta_c \to K^+K^-\eta$ and $\eta_c \to K^+K^-\pi^0$ in two-photon interactions*, Phys. Rev. **D89** (2014) 112004, arXiv:1403.7051.

[2] Belle collaboration, Q. N. Xu *et al.*, *Measurement of $\eta_c(1S)$, $\eta_c(2S)$ and non-resonant $\eta'\pi^+\pi^-$ production via two-photon collisions*, Phys. Rev. **D98** (2018) 072001, arXiv:1805.03044.

[3] V. V. Anashin *et al.*, *Measurement of $J/\psi \to \gamma\eta_c$ decay rate and η_c parameters at KEDR*, Phys. Lett. **B738** (2014) 391, arXiv:1406.7644.

[4] BESIII collaboration, M. Ablikim *et al.*, *Measurements of the mass and width of the η_c using $\psi' \to \gamma\eta_c$*, Phys. Rev. Lett. **108** (2012) 222002, arXiv:1111.0398.

[5] LHCb collaboration, R. Aaij *et al.*, *Measurement of the $\eta_c(1S)$ production cross-section in proton-proton collisions via the decay $\eta_c(1S) \to p\overline{p}$*, Eur. Phys. J. **C75** (2015) 311, arXiv:1409.3612.

[6] LHCb collaboration, R. Aaij *et al.*, *Study of charmonium production in b-hadron decays and first evidence for the decay $B_s^0 \to \phi\phi\phi$*, Eur. Phys. J. **C77** (2017) 609, arXiv:1706.07013.

[7] LHCb collaboration, R. Aaij *et al.*, *Observation of $\eta_c(2S) \to p\overline{p}$ and search for $X(3872) \to p\overline{p}$ decays*, Phys. Lett. **B769** (2017) 305, arXiv:1607.06446.

[8] Particle Data Group, M. Tanabashi *et al.*, *Review of Particle Physics*, Phys. Rev. **D98** (2018) 030001.

[9] Y. Feng *et al.*, *Phenomenological NLO analysis of η_c production at the LHC in the collider and fixed-target modes*, Nucl. Phys. **B** (2019) 114662, arXiv:1901.09766.